

NUMERICAL SIMULATION OF URBAN CLIMATE IN HANSHIN DISTRICT USING REMOTE SENSING DATA

KENJI TAKAGI¹, KENSUKE KITADA¹, RYUZOU OOKA²,
YOUICHI KAWAMOTO², HITOSHI WATANABE²
AND SATOSHI MIYASAKA³

¹Kajima Technical Research Institute, ²University of Tokyo,

³Nakanihon Air Service Co., LTD.

ABSTRACT

This paper first describes the preparation of data relating to atmospheric conditions of areas of land (hereafter referred to as land covering data) using records obtained from a Multi-Special Scanner (MSS) which was fitted to an aircraft. Next, the results of simulations of the atmospheric conditions over the Hanshin district obtained from a meso-scale numerical simulation of the atmosphere based on these data are explained. In this paper, the effects of the results obtained from the land covering data on the atmospheric simulation are investigated using the digital national land information and detailed digital information both of which are usually applied for a meso-scale atmospheric simulation in addition to the data obtained from the MSS. Finally, the ground surface temperature and the thermal environment in the vicinity of the ground surface are simulated by heat balance analyses at the ground surface (hereafter referred to as heat balance analyses) with consideration to vegetation and block shapes. Through comparing the simulation results with the ground surface temperature computed using the thermal infrared pictures obtained from the MSS, the results of the investigation of the simulation accuracy are described.

As a result, it was made clear that the atmospheric conditions as well as the ground surface temperature can be simulated more accurately by using the MSS data than by using any other data and that the urban climate on a fine day in the summer can be simulated well within a margin of ± 2 and ± 4 for the atmospheric temperature and the ground surface temperature respectively

1. INTRODUCTION

Recently, in the large cities of Japan heat-island phenomena are raising serious questions. Studies on analyses of the heat-island phenomena by means of numerical simulations have been carried out by various research groups. (Kim et. al., 2000, Hagishima et. al., 2001, Harayama et. al., 2001, Narumi et. al., 2002) In order to improve the accuracy of any simulation, the precision of the input land covering data is as important as

numerical simulation models and numerical computation methods. In this paper, numerical simulations of the Hanshin district were carried out using the data obtained from the MSS, the national land numerical data and detailed numerical data in order to investigate the effects of the differences in the land covering data on the results of the meso-scale atmospheric simulation.

Furthermore, for the purpose of simulating a more detailed thermal environment by conducting meso-scale atmospheric simulations, heat balance analyses with consideration to vegetation and block shapes were carried out. The ground surface temperature simulated for the horizontal resolution of 100m was compared to the ground surface temperature distribution computed from the thermal infrared pictures in the MSS data.

2. LAND COVERING DATA AND GROUND SURFACE TEMPERATURES TAKEN FROM MSS DATA

The MSS is an observation device which can separate the sunlight reflected and radiated from the ground into multi-wavelengths. The equipment outline, observation outline and the observation area are shown in Tables 1 and 2 and Fig.1 respectively. Corrections of the MSS data resulting from the observation system and corrections according to the topographical map were carried out. The land covering data were obtained by classifying the conditions relating to areas of land with a method of supervised classification (a method of maximum likelihood) using the visible bands and near-infrared band data.

Moreover, ground surface temperature distribution data were prepared based on the infrared band data by carrying out temperature corrections using the ground surface temperature obtained from observations made using radial thermometers located at several places over the ground. The ground observations and the aircraft observations were carried out simultaneously.

Table 1: Observation outline

Research area (Fig.1)	Suita City
Research date	Aug.26, 2002
Observation period	11:43~12:32
Observation altitude	About 3,200m above sea level
Space resolution	4m
Weather during observations	Fine weather;temperature 34.2 Osaka Metrological Observatory

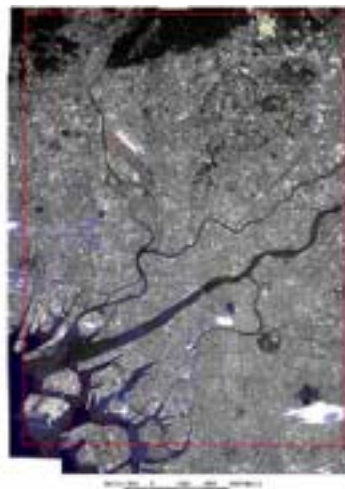


Fig. 1: Observation areas for MSS

Table 2: Outline of MSS

Observation equipment	AZM
Detected band number	43 bands
Collecting channel number	12 or 24 (switching: selection from 43 bands)
Instantaneous visual field angle	1.25 or 2.5 mrad (switching)
Scanning angle	80 °
Scanning speed	74 rotations/sec
Position control	2 axes movable mount and rolling
Quantization level	14bit+2bit offset (2byte)
Measurement temperature range	Low temperature range -20~+100 High temperature range -20~+500
Recording method	PCM, VHS type VLDS

3. SIMULATION OF ATMOSPHERIC CONDITIONS BY MESO-SCALE ATMOSPHERIC NUMERICAL SIMULATION

3.1 Numerical simulation method

The meso-scale analysis function of the Software Platform (Mochida, et. Al., 2000) was used for the meso-scale atmospheric simulation. Fig.2 shows the areas subjected to the analyses. The nested grids of 3 steps shown in Table 3 were established in these areas. The atmosphere up to an altitude of 9.6km above the ground was divided into 49 meshes at varying intervals in a vertical direction for the three grids. The soil up to a depth of 1m under ground was divided into 5 meshes at varying intervals. The analyses were carried out from 00:00 on Aug. 26 through 00:00 on Aug.27.

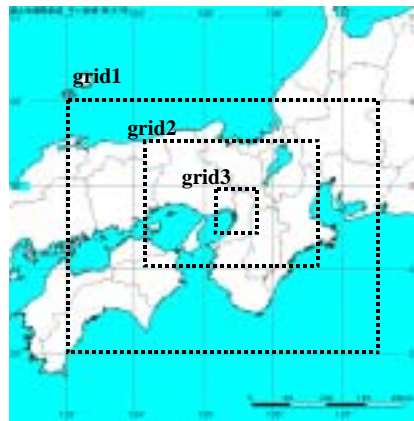


Figure 2: Areas subjected to analyses

Table 3: Analysis area

	Computation area (x × y × z km)	Mesh divided number	Width of horizontal mesh (km)
Grid 1	450 × 450 × 9.6	45 × 45 × 49	8
Grid 2	200 × 180 × 9.6	50 × 45 × 49	4
Grid 3	40 × 43 × 9.6	40 × 43 × 49	1

Table 4: Setting condition

Item	Detail
Time integral step breadth t	Grid 1:30 sec, grid 2:15sec, grid 3:2.5sec
Weather	Amount of cloud is established as 1.
Initial temperature profile	Temperature = 26 at 0.0m above sea level Z1<5000m: = 0.0050 K/m Z1>5000m: = 0.0040 K/m
Artificial exhaust of heat	Roads: 100W/m ² Building: 50W/m ²
Initial humidity profile	McClatchey's model made by setting relative humidity of ground surface at 70%.
Turbulence length scale	Established using Blackadar equation: $l=kz/(1+kz/l_0)$

As for the atmospheric conditions at places subjected to the analyses, the wind direction and the wind speed were set as a southerly wind moving at 1m/sec at an altitude of 9.6km above the ground. The sea ground surface temperature was set at 28 which does not change according to the passage of time. This temperature was decided upon using actual measured values. Other conditions are shown in Table 4.

3.2 Land covering data

With regard to the land covering data for grid 1 and grid 2, ground surface parameters were computed from the digital national land information. As for those for grid 3, ground surface parameters based on three different data as shown in Table 5 were computed.

Table 5: Land covering data

Case1	Case 2	Case 3
Digital national land Information	Detailed digital information	MSS data
Rice fields	Rice fields	
Fields	Fields, other farmlands	Grasslands
Fruit orchards		
Wooded areas		
Forests	Forests and Wastelands	Trees
Wasteland	Residential areas under construction	Fire burnt areas and Bare land
Built-up areas	Industrial use Ordinary low storied houses Densely packed houses Middle and high storied buildings Commercial and business use Public facilities	Structures
Principal transportation areas	Roads	Asphalt
Lands for other use	Parks, Green zones and others	Concrete
Drainage areas	Rivers and lakes	Water surface
Coastal areas		
Seawater areas	Sea	
Areas of obscurity		Clouds and Shadows

3.3 Results of simulations

Fig.3 shows the ground surface temperature in grid 2 at 12:00 on Aug.26 and the wind speed distribution at a height of 10m above the ground. Figs.4 and 5 illustrate the results of the measurements at the AMeDAS observation points (Takebayashi, 2001).

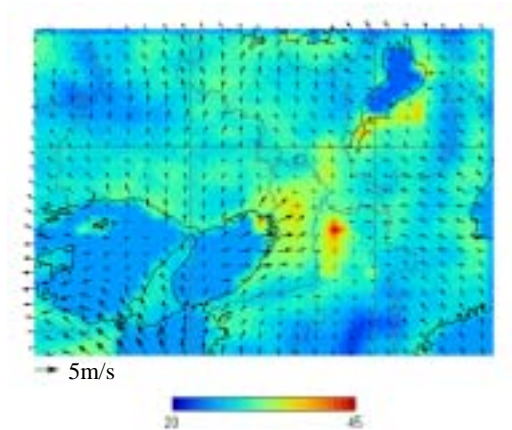


Figure 3: Surface temperatures and wind speeds distribution at a height of 10m above ground (At 00:00 on Aug.26, grid2)



Figure 4: Observation results of Wind distribution (At 00:00 on Aug.1, 1995)



Figure 5: Observation results of Wind distribution (Average at 00:00 on fine days in July, Aug and Sep., 1995)

Those results were obtained under the same weather conditions as those for the computation. As a result, the sea wind above Osaka Bay can be

simulated quite well. In particular, it can be seen that the wind strongly blows into urban districts whose ground surface temperature is high. This phenomenon corresponds fairly well to the AMeDAS observation data (Figs.4,5).

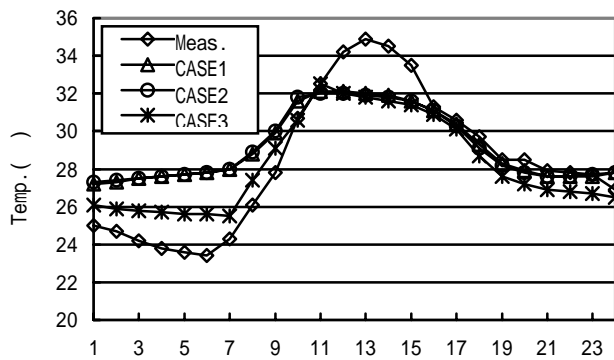


Figure 6: Transition of temperatures (Osaka District Meteorological Observatory)

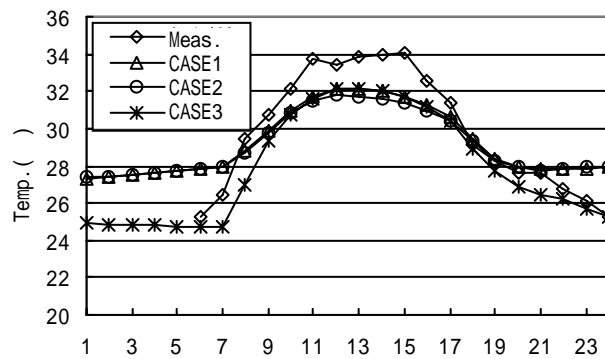


Figure 7: Transition of temperatures (Memorial Park in Amagasaki City)

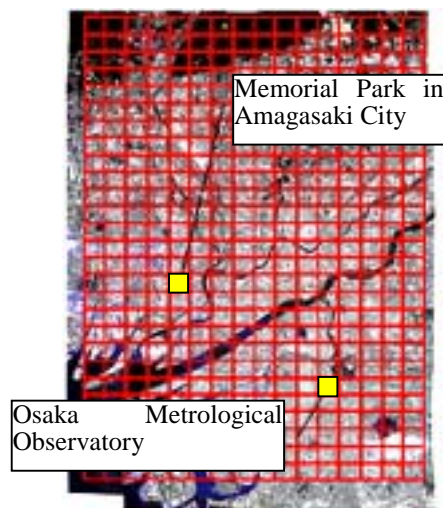


Figure 8: Weather observation points

Figures.6 and 7 illustrate the transition of the air temperature at height 10m in each case for grid 3. Fig.6 shows the observed values and the

analysis values at the Osaka District Metrological Observatory. Fig.7 shows the observed values and the analysis values at the Memorial Park in Amagasaki City. The analysis value is the mean value for the subjective meshes. Fig. 8 shows the location of the mesh for Osaka and Amagasaki.

An obvious difference in the change in the temperature can be seen between the observed value and the analysis value. In particular, in cases 1 and 2 the difference in the temperature is about 4 °C at maximum. Any change in the temperature over the course of a day is small as a whole. Among the analysis results, results for case 3 obtained using the MSS data correspond best to the change in the observed value and the difference is about 2 °C at maximum. In each case, analyses were carried out under the same conditions except for land-use data. Therefore, the results showing the effects of the change in input data are conspicuous.

4. SIMULATION OF THERMAL ENVIRONMENT IN THE VICINITY OF GROUND SURFACE BY HEAT BALANCE ANALYSES WITH CONSIDERATION TO VEGETATION AND BLOCK SHAPES

4.1 Simulation method for heat balance at the ground surface

In order to analyze a more detailed thermal environment in the vicinity of the ground surface, heat balance analyses are carried out using the results of the simulation carried out in the previous chapter. In the heat balance analyses, the heat balance at the ground surface, which was classified according to the conditions covering areas of land, and the underground thermal transfer are computed simultaneously under the consideration that both are uniform in a horizontal direction. The underground thermal transfer is computed based on the one dimensional heat conduction equation in a vertical direction.

$$HC_g \frac{\partial T_g}{\partial t} = \frac{\partial}{\partial z} \left[\lambda \frac{\partial T_g}{\partial z} \right] \quad (1)$$

Where HC_g : Thermal capacity of soil (J/m³), T_g : Underground temperature (K), λ : Underground thermal conductivity (W/Mk)

The conditions covering areas of land are classified into 10 categories based on the MSS data. $Flhg$, heat energy flux (W/m²) which represents for the atmosphere, is provided as a ground surface boundary condition for the computation of the underground thermal transfer.

$$Flhg = \left[\lambda \frac{\partial T_g}{\partial z} \right]_{z=0} = \sum_k^{kn} a_k Flhg_k \quad (2)$$

Where $Flhg_k$: Heat energy flux for each category, a_k : Area ratio accounted for by category k

The heat energy flux in each category is computed using three kinds of computation models; a thermal change model for a boundary surface such as an area of bare land and a water surface, a vegetation model with consideration to layers of plants and an urban canopy model with

consideration to block shapes. (Yoshida et. Al., 2001, Deardorff, 1987, Kimura et. Al., 1991)

4.2 Input data

The MSS data are used for the land covering data which are the basis of the computations. The area ratio in the mesh of 100m for each of the 10 categories is used for the land covering data.

As shown in Fig.9, three areas which have certain geographical characteristics in the environs of Osaka City located in the analysis area of grid 3 for the atmospheric simulation were selected for the computation. They were the northern area with a relatively large number of mountains and forests (area R1), Suita City where buildings and houses stand close together (area R2) and the water front area facing Osaka Bay (area R3).

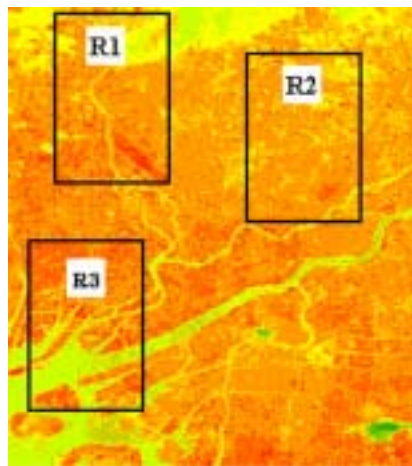


Figure 9: Computation areas on the ground surface

The computation value of the meso-scale atmospheric simulation was used for weather conditions of the upper atmosphere. The data used were the temperature at a height of 10m above the ground, absolute humidity, wind speed, sunshine amount reaching the ground and the radiation level in the atmosphere. The data obtained every 24 hours were interpolated linearly in time and space.

4.3 Computation results

Fig.10 shows the correlation between the computation value and the measurement value both of which were obtained from the mesh of 100m. The value for the ground surface temperature shown on the abscissa is the fourth power mean value of the ground surface temperature in each category of the mesh of 100m obtained on the basis of the category area ratio. Although the difference in the ground surface temperature for each mesh is about 10 at maximum, the computation value simulates the measurement value to a good degree.

Table 6 shows the comparison between the measurement value and the regional mean value of the computation value for the ground surface

temperature in each category. The ground surface temperature T_k for each category was obtained from the ground surface temperature Tg_i using the following equation for each mesh of 100m.

$$T_k = \frac{\sum_i^N a_{ki} Tg_i}{\sum_i^N a_{ki}} \quad (3)$$

Where N : Total number of meshes in a computation region

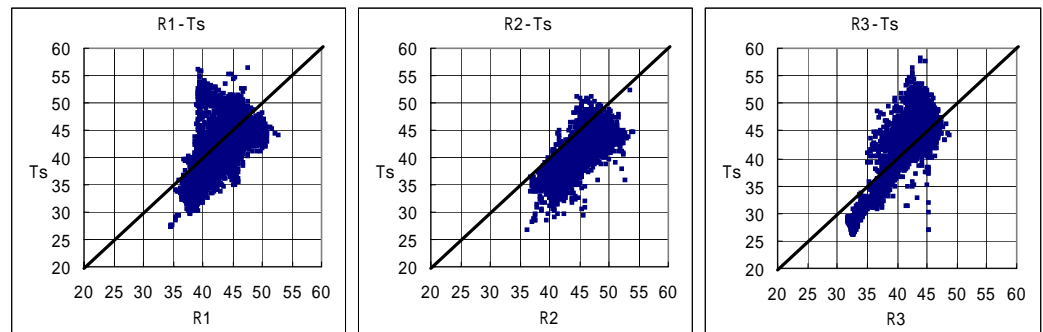


Figure 10: Co-relation of measurement values and computation values

Table 6: Comparison of measurement values and computation values for each category (unit: $^{\circ}\text{C}$)

	Structures	Shadows	Trees	Grasslands	Asphalt	Bare ground	Concrete	Water surface	Area average
Area Ratio (R1)	30.4	0.6	16.0	21.7	20.9	7.8	1.6	1.1	
Computed	44.8	44.7	39.4	42.5	45.6	44.8	47.1	39.3	43.6
Measured	45.1	43.9	35.6	42.4	44.9	44.2	44.8	34.9	42.8
Difference	-0.3	0.9	3.8	0.1	0.7	0.6	2.3	4.4	0.8
Area Ratio (R2)	33.0	0.7	11.6	11.0	36.5	5.9	0.0	1.3	
Computed	46.8	46.1	42.5	44.3	47.2	47.2	0.0	41.7	46.1
Measured	43.7	42.3	39.3	40.2	43.4	42.9	0.0	34.5	42.5
Difference	3.1	3.9	3.2	4.1	3.9	4.3	0.0	7.3	3.6
Area Ratio (R3)	32.1	1.6	1.3	4.2	24.1	8.7	2.2	25.3	
Computed	43.1	41.3	40.6	40.3	43.5	42.3	43.4	33.2	40.5
Measured	46.3	41.7	43.1	43.6	45.3	44.7	45.2	29.9	41.5
Difference	-3.2	-0.4	-2.5	-3.2	-1.8	-2.4	-1.8	3.4	-1.0

Although there is a difference according to the region subjected to the computation, the ground surface temperature is simulated with a margin of ± 4 by the heat balance analyses. In regions R1 and R2, the computation value is high. On the contrary, in region R3 located near the sea the measurement value is low. It can be thought that this is so because the effects of the sea wind and the surface of the water are overestimated in the simulation.

5. CONCLUSION

Meso-scale atmospheric simulations for Hanshin district as urban areas were carried out using the national land numerical data, detailed numerical data and the MSS data for the land-use. Simulation results obtained by using the MSS data among the three kinds of data for land-use qualitatively agreed with the measurement value and the atmospheric temperature could be simulated with an accuracy of ± 2 .

Furthermore, in order to simulate a more detailed thermal environment in the vicinity of the ground surface using the results of the meso-scale atmospheric simulation to which the MSS data were applied, heat balance analyses were conducted. The analysis results were compared with the ground surface temperature obtained by using the MSS data. As a result, the ground surface temperature which has a large variation in time and space could be simulated with an accuracy of ± 4 .

REFERENCES

- Mochida, A., Murakami, S., Kim, S.J., Kondo, H., Shimada, A. and Ooka, R., 2000. Development of software platform for total analysis of urban heat island (Part1). *Summaries of Technical papers of annual meeting architectural institute of Japan*, D-1,1099-1100.
- Takebayashi, H., Moriyama, M., Murakami, S., Ooka, R., Mochida, A., Shibaike, H. and Yoshida, S., 2001. Urban scale climate analysis using calculation results by numerical simulation model and observation data. *Journal of Architecture, Planning and Environmental Engineering*, 556, 63-68.
- Kim, S. et al., 2000. Study on Effects of Urbanization on Urban Climate in Kanto Plane. *Journal of Architecture, Planning and Environmental Engineering*, 534, 83-88.
- Hagishima, A. et al., 2001. An Organic Analysis for Quantitative Estimation of Heat Island by the Revised Architecture-Urban-Soil-Simultaneous Simulation Model, (AUSSSM). *Journal of Architecture, Planning and Environmental Engineering*, 550, 79-86.
- Harayama, K. et al., 2001. Numerical Study Based on Unsteady Radiation and Conduction Analysis. *Journal of Architecture, Planning and Environmental Engineering*, 556, 99-106.
- Narumi, D. et al., 2002. Effect of Anthropogenic Waste Heat Upon Urban Thermal Environment. *Journal of Architecture, Planning and Environmental Engineering*, 562, 97-104.
- Yoshida, M., Oota, K. and Takagi, K., 2001. Models of Ground Surface and Cloud to Estimate the Planetary Boundary layer. *Kajima Technical research Institute Annual Report*, 49, 189-194.
- Deardorff, J. W., 1987. Efficient Prediction of Ground Surface Temperature and Moisture, with Inclusion of a Layer of Vegetation. *Journal of Geophysical Research*, 1889-1903.
- Kimura, F. and Takahashi, S., 1991. The Effects of Land-use and Anthropogenic Heating on the Surface Temperature in Tokyo Metropolitan Area, *Atmospheric Environment*, 25B-2, 156-164.